

Deep Argumentative Explanations

Emanuele Albini, Piyawat Lertvittayakumjorn, Antonio Rago & Francesca Toni

Department of Computing, Imperial College London, UK

{ emanuele, pl1515, a.rago, ft }@imperial.ac.uk

Abstract

Despite the recent, widespread focus on eXplainable AI (XAI), explanations computed by XAI methods tend to provide little insight into the functioning of Neural Networks (NNs). We propose a novel framework for obtaining (local) explanations from NNs while providing transparency about their inner workings, and show how to deploy it for various neural architectures and tasks. We refer to our novel explanations collectively as *Deep Argumentative eXplanations* (DAXs in short), given that they reflect the *deep* structure of the underlying NNs and that they are defined in terms of notions from *computational argumentation*, a form of symbolic AI offering useful reasoning abstractions for explanation. We evaluate DAXs empirically showing that they exhibit *deep-fidelity* and low computational cost. We also conduct human experiments indicating that DAXs are comprehensible to humans and align with their judgement, while also being competitive, in terms of user acceptance, with some existing approaches to XAI that also have an argumentative spirit.

1 Introduction

Several recent efforts in AI are being devoted to explainability, in particular of black-box methods such as deep learning. However, the majority of explanation methods in the literature (e.g., see overview in [Guidotti *et al.*, 2019]) focus on describing the role of inputs (e.g., features) towards outputs. A consequence of such “flat” structure of explanations is very little transparency on how the outputs are obtained. This focus on the “flat”, functional, input-output behaviour also disregards the human perspective on explanations and the potential benefits for XAI from taking a social science viewpoint [Miller, 2019].

To address these issues when explaining predictions by *Neural Networks (NNs)*, we propose *Deep Argumentative eXplanations (DAXs)*, based on concepts drawn from the field of Computational Argumentation in symbolic AI (see overview in [Atkinson *et al.*, 2017]).

Argumentative models of explanation are advocated in the social sciences, e.g., in [Antaki and Leudar, 1992], as suitable

to humans. Indeed, the explanations generated by some existing methods have an argumentative spirit, e.g., LIME [Ribeiro *et al.*, 2016] and SHAP [Lundberg and Lee, 2017] assign to input features importance scores towards outputs, giving a form of weighted pro/con evidence. Computational argumentation is particularly suitable for underpinning argumentative explanations. It is a mature field with solid foundations, offering a variety of *argumentation frameworks* comprising sets of arguments and *dialectical relations* between them, e.g., of *attack* (cf. con evidence), as in [Dung, 1995], and/or *support* (cf. pro evidence), as in [Cayrol and Lagasquie-Schiex, 2005]/[Amgoud and Ben-Naim, 2016], resp. In these frameworks, arguments may be chained by dialectical relations forming potentially deep (debate) structures. In some such frameworks, starting from [Dung, 1995], anything may amount to an argument, so long as it is in dialectical relation with other arguments (e.g., strategies in games can be seen as arguments [Dung, 1995], and, in our DAXs, neurons and groups thereof in NNs may be understood as arguments). Further, in computational argumentation, debates (i.e., argumentation frameworks) can be analysed using so-called semantics, e.g., amounting to definitions of *dialectical strength* satisfying desirable *dialectical properties* (such as that attacks against an argument should decrease its dialectical strength [Baroni *et al.*, 2018]). When argumentation frameworks are extracted for the purpose of explaining underlying methods (e.g., recommenders, as in [Rago *et al.*, 2018]) a semantics is drawn from quantities computed by the underlying methods (e.g., predicted ratings in [Rago *et al.*, 2018]) insofar as they satisfy relevant dialectical properties.

Figure 1 gives a simple illustration, for a toy feed-forward NN (FFNN), of our framework (see Section 3 for details). In a nutshell, DAXs (in various formats, e.g., conversational as in Figure 1) are extracted from (instances of) *Generalised Argumentation Frameworks* (GAFs) potentially including any number and type of dialectical relations (e.g., attack and support, as in Figure 1). These frameworks consist of directed links between (groups of) neurons (treated as arguments) relevant to the NN prediction in needs of explanation. GAFs are extracted so that arguments therein are equipped with a dialectical strength given by quantitative measures derived from the underlying NNs, e.g., in one of the DAX instances we propose, given by Layer-wise Relevance Propagation (LRP) [Bach *et al.*, 2015]), governed by desirable dialectical prop-

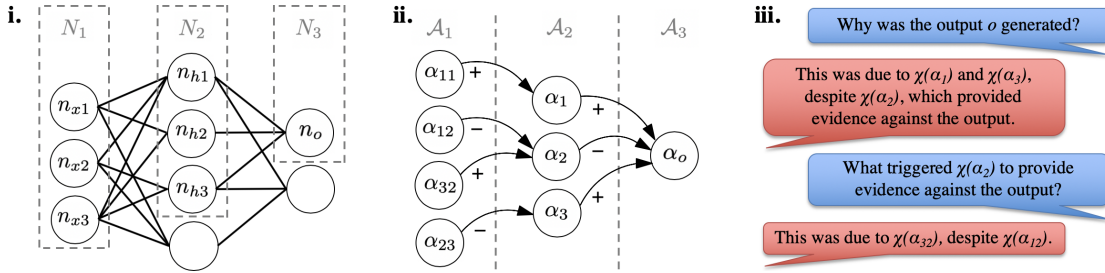


Figure 1: (i) Toy feed-forward NN (FFNN), with input/hidden/output neurons selected as nodes labelled with subscript $x/h/o$, resp., and layers N_1, N_2, N_3 ; (ii) extracted Generalised Argumentation Framework (GAF) with dialectical relations of attack (indicated with $-$) and support (indicated with $+$); and (iii) example DAX generated from the GAF (with a conversational format, comprising user (right) and system (left) statements). Here, χ (a hyper-parameter in our framework) indicates a representation, amenable to user consumption, for arguments in the GAF, dependent on the cognitive abilities and needs of the target users.

erties identified up-front to fit the setting of deployment for the given NNs/tasks.

Our contribution in this paper is threefold: (1) we give the general DAX framework and three concrete instances thereof, varying the underlying NN, the GAFs, how their semantics is derived from the underlying NNs, the dialectical properties it satisfies, and the format in which DAXs are delivered to users; (2) we evaluate the three instances empirically, showing that they exhibit a property that we term *deep-fidelity* and that they have low complexity; (3) we conduct experiments with humans showing some of DAXs' advantages: comprehensibility to humans and alignment with their judgement, as well as, in comparison with LIME and SHAP (selected due to their argumentative spirit), their increased ease of understanding, insightfulness, and capability of inspiring trust.

Although several works exist for argumentation-based explanation, e.g., [Briguez *et al.*, 2014; Rago *et al.*, 2018], to the best of our knowledge DAXs are the first for NNs. We plan to release the DAX toolkit upon acceptance.

2 Background and Related Work

Neural Networks (NNs). For our purposes a (trained) NN \mathcal{N} can be seen as a directed graph whose nodes are neurons and whose edges are connections between neurons, formally \mathcal{N} is $\langle V, E \rangle$ with V a set of neurons and $E \subseteq V \times V$ a set of directed edges. Different neural architectures impose different restrictions on these graphs (e.g., in the FFNN in Figure 1i, neurons are organised in strata with each neuron connected to every neuron in the next stratum). Independently of the architecture, neurons in a trained NN are equipped with activation values (computed by some activation function) and links are equipped with weights (learnt during training).¹

Computational argumentation. DAXs are obtained from Generalised Argumentation Frameworks (GAFs), e.g., as understood in [Gabbay, 2016]. Formally, these are tuples $\langle \mathcal{A}, \mathcal{R}_1, \dots, \mathcal{R}_m \rangle$ with \mathcal{A} a set (of *arguments*), $m \geq 1$ and, $\forall i \in \{1, \dots, m\}, \mathcal{R}_i \subseteq \mathcal{A} \times \mathcal{A}$ is a binary, directed *dialectical*

¹Note that, given that we focus on explaining trained NNs, we ignore here how training is performed, and how performant the trained NNs are. Also, for simplicity we ignore biases in the formalisations in the paper.

relation. Intuitively, GAFs are abstractions of debates, with arguments representing opinions and dialectical relations expressing various forms of agreement (support) or disagreement (attack) between opinions. GAFs can also be seen as directed graphs (as in Figure 1ii), with arguments as nodes and dialectical relations as labelled edges. Various instances of GAFs have been studied for specific choices of dialectical relations. A well-studied instance is *abstract argumentation frameworks* [Dung, 1995] with $m = 1$ and $\mathcal{R}_1 = \mathcal{R}^-$ is attack. We will use *support argumentation frameworks* (SAFs) [Akgoud and Ben-Naim, 2016], where $m = 1$ and $\mathcal{R}_1 = \mathcal{R}^+$ is support; *bipolar argumentation frameworks* (BAFs) [Cayrol and Lagasquie-Schiex, 2005], where $m = 2$, $\mathcal{R}_1 = \mathcal{R}^-$ is attack, $\mathcal{R}_2 = \mathcal{R}^+$ is support; and a form of *tripolar argumentation frameworks*, where $m = 3$. We will also use semantics given by mappings $\sigma : \mathcal{A} \rightarrow \mathcal{V}$ for evaluating arguments' *dialectical strength* over a set of values \mathcal{V} [Baroni *et al.*, 2018], (in this paper $\mathcal{V} = \mathbb{R}$ and σ is extracted from trained NNs). Finally, we will use (existing and novel) *dialectical properties*, in the spirit of [Baroni *et al.*, 2018], that σ needs to satisfy to ensure that the GAFs have natural features of human debates (e.g., that strong attacks decrease the strength of opinions).

XAI approaches. Amongst the many proposals (e.g., see survey in [Guidotti *et al.*, 2019]), some are model-agnostic (e.g., LIME [Ribeiro *et al.*, 2016], SHAP [Lundberg and Lee, 2017]), while others are tailored to specific methods (e.g., for NNs, LRP [Bach *et al.*, 2015], Grad-CAM [Selvaraju *et al.*, 2020], GRACE [Le *et al.*, 2020]), but all generate “flat” explanations, in terms of input features only, without indicating how.

We will compare DAXs with LIME and SHAP in our human experiments, and will use LRP and Grad-CAM to compute dialectical strength in some of our proposed DAX instantiations. In a nutshell, LIME and SHAP compute (using different methods) positive and negative attribution values for input features, when explaining outputs by any classifier (the details of these computations are not important here). For both methods, the computed (positive and negative) attribution values can be seen as arguments (for and against, resp., the output prediction). This argumentative spirit of LIME and SHAP is the reason why we choose to compare them with DAXs in the human evaluation. LRP is a technique for interpretability which is able to scale to highly complex NNs: it

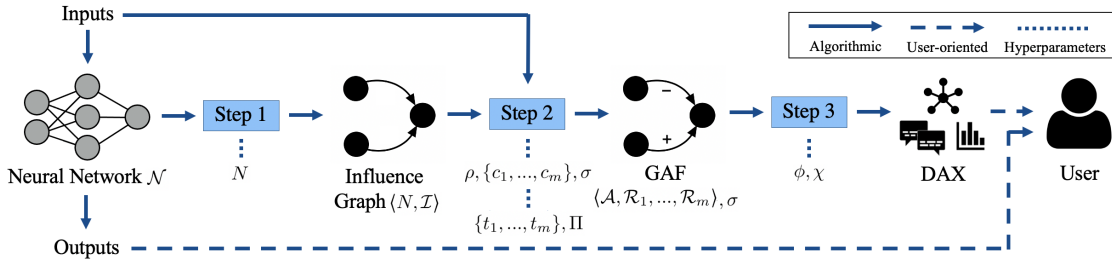


Figure 2: DAX framework (alongside the typical process of obtaining outputs from a neural model given its inputs) comprising steps: 1. Based on the chosen nodes N within \mathcal{N} , extract $\langle N, \mathcal{I} \rangle$, a directed graph of influences between nodes. 2. Extract a GAF from the output of the first step, based on choices of argument mapping ρ , relation characterisations $\{c_1, \dots, c_m\}$ and dialectical strength σ . These choices are driven by the types of relations $\{t_1, \dots, t_m\}$ to be extracted and the dialectical properties Π that σ should satisfy (on the GAF) to form the basis for explanations. 3. Generate a DAX from the GAF and dialectical strength σ , for user consumption in a certain format ϕ , associating arguments with human-interpretable concepts through a mapping χ .

operates by propagating a prediction backwards in the NN, using a set of purposely designed propagation rules (specifically we use LRP-0 [Bach *et al.*, 2015]). Grad-CAM uses the gradients of any target concept (e.g., “dog”) flowing into the final convolutional layer of a CNN for image classification to produce a coarse localisation map highlighting the important regions in the input image for predicting the concept.

Some explanation methods, like DAXs, make use of symbolic representations, e.g., ordered decision diagrams in [Shih *et al.*, 2018] and logical representations in [Ignatiev *et al.*, 2019]. These methods also focus on input-outputs only and are “flat”. Computational argumentation is used by many for explanation purposes (e.g., in [Naveed *et al.*, 2018]). Various neural architectures have also been used for argument mining from text [Lippi and Torroni, 2016], in some cases to extract GAFs [Cocarascu *et al.*, 2020], but not for the purposes of explanation.

Some recent methods generate “structured” explanations, including hierarchical explanations [Chen *et al.*, 2020] and explanations exploiting dependencies [Aas *et al.*, 2019]. These incorporate interactions between input features only, so they can also be deemed “flat” in our sense.

Some works, like DAXs, move away from “flat” explanations, predominantly with images: in [Wang and Nasconcelos, 2019] regions of an image generating insecurities between two outputs are highlighted, thus unearthing some of the “deliberative” reasoning behind the outputs (but still focusing on input features); network dissection [Bau *et al.*, 2017] identifies regions of an image activating certain filters in a Convolutional NN (CNN), giving these filters a semantic meaning; self-explaining NNs [Alvarez-Melis and Jaakkola, 2018] use one NN for classification and another for explanation, to obtain explanations based on higher-level features/concepts and their relevance towards a classification; in [Olah *et al.*, 2018] positive/negative connections between concepts are extracted from neurons in a CNN. There are promising steps, but focus on visualisation, falling short of a general framework for explanations showing the interplay amongst inputs, intermediate layers and outputs.

Several works advocate the need for evaluating explanations (e.g., see overview in [Sokol and Flach, 2020]) in several

ways. We consider the computational cost (of obtaining DAXs from trained NNs), commonly used in the literature [Sokol and Flach, 2020], as well as a novel property of *deep-fidelity*, evaluating it empirically for our proposed DAX instances.

A user-driven perspective on explanations is advocated by many [Miller, 2019], as is the fact that different explanation styles, as envisaged by DAX, may need to be considered to aid transparency and trust and to support human decision making (e.g. see [Rader *et al.*, 2018; Kunkel *et al.*, 2019]). In the same spirit, we conduct a human study on a DAX instance.

3 DAX Framework

Here, we outline our general DAX framework for explaining NN predictions. Throughout, we use the example in Figure 1 for illustration, and otherwise assume as given a generic, trained NN \mathcal{N} for prediction, with explanations needed for an output o computed by \mathcal{N} for given input x , where o is a single classification, e.g., the most probable class in the output layer of \mathcal{N} . For the purpose of explaining o for x , \mathcal{N} amounts to a function f such that $f(x) = o$ and can be equated to a directed graph $\langle V, E \rangle$ (as described in Section 2).

DAXs are constructed in 3 steps, as outlined in Figure 2 and described below, with a focus on the choices (hyperparameters) that need to be instantiated when DAXs are deployed.

Step 1: from NNs to influence graphs. This amounts to determining, within \mathcal{N} , an influence graph $\langle N, \mathcal{I} \rangle$ with a set N of nodes and a set \mathcal{I} of influences as candidate elements of (binary) dialectical relations of the GAF (to be identified at Step 2) underlying explanations for why $f(x) = o$. The choice of N within V is a hyper-parameter dictated by the setting of deployment. We will see that in some instantiations of DAX $N \subseteq V$, whereas in others nodes in N may also include groups of neurons in V . Note that, in principle, N may be exactly V but in practice it will need to be considerably smaller, to accommodate the cognitive needs of users. Once N has been chosen, we obtain \mathcal{I} automatically as follows:

Definition 1 Let hyper-parameter $N \subseteq V \cup \mathcal{P}(V)$ be given. Then, the influence graph $\langle N, \mathcal{I} \rangle$ is such that $\mathcal{I} = \{(n_1, n_2) | n_1, n_2 \in N \text{ and there is a path in } \langle V, E \rangle \text{ from (a neuron in) } n_1 \text{ to (a neuron in) } n_2\}$.

Practically, N will include (groups of) neurons in the input layer of \mathcal{N} , the neuron n_o in the output layer responsible for output o as well as any desired (groups of) neurons from the hidden layers. For example, if \mathcal{N} is a CNN, then N may consist of the neurons in the input layer, n_o as well as all the the neurons of the max-pooling layer (as for the DAX instances for text, in Section 4) or all filters in the last convolutional layer (as for the DAX instance for images, in Section 4). Both choices (as well as several other “semantically meaningful” alternatives) reflect the inner structure of the underlying NN.

In all DAX instances in this paper, we choose $N = N_1 \cup \dots \cup N_k$, for $k > 2$, with $N_k = \{n_o\}$ and N_1, \dots, N_k disjoint sets of nodes such that for every $(n_1, n_2) \in \mathcal{I}$ there exists $i \in \{1, \dots, k-1\}$ with $n_1 \in N_i, n_2 \in N_{i+1}$. Thus, N_1, \dots, N_k amount to *strata*, contributing (in Steps 2 and 3) to *deep* explanations, where (arguments representing) nodes in each stratum are explained in terms of (arguments representing) nodes in the previous stratum. For illustration, given the FFNN in Figure 1i, N amounts to all neurons in V with a path to n_o , arranged in three strata to match the three layers of the FFNN. Note that, in general, depending on the choice of N , strata may result from non-adjacent layers in \mathcal{N} . Also, although the choice of N (and thus \mathcal{I}) is tailored to explaining $f(x) = o$, differently from our earlier illustration the choices from the hidden layers of the given \mathcal{N} can be made a-priori, independently of any input-output pair, and then instantiated for each specific input-output pair (this is exactly what we do in the DAX instances in Section 4, to guarantee a low computational cost, as discussed in Section 5).

Step 2: from influence graphs to (dialectical property-compliant) GAFs. This amounts to extracting a GAF $\langle \mathcal{A}, \mathcal{R}_1, \dots, \mathcal{R}_m \rangle$ from $\langle N, \mathcal{I} \rangle$, with arguments drawn from the nodes in N and dialectical relations drawn from the influences in \mathcal{I} . This requires, first and foremost, the choice (hyper-parameter) of the number of dialectical relations (m) and their *relation types* t_1, \dots, t_m . For illustration, In Figure 1ii the GAF is a BAF with two dialectical relations with relation types attack (-) and support (+). The choice of the types indicates that the envisaged DAXs will be defined in terms of (dis)agreement between nodes (i.e., neurons or groups thereof).

The extraction of arguments is driven by a (hyper-parameter) mapping $\rho : \mathcal{A} \rightarrow N$ such that $\mathcal{A} = \mathcal{A}_1 \cup \dots \cup \mathcal{A}_k$ and for each $\alpha \in \mathcal{A}_i$ there is exactly one $n \in N_i$ with $\rho(\alpha) = n$ (we say that α represents n and that \mathcal{A}_i represents N_i). For illustration, in Figure 1ii all nodes in N contribute at least one argument, with n_{x1} contributing two arguments, and all other nodes contributing exactly one argument. Thus, $\rho(\alpha_{ij}) = n_{xi}$, $\rho(\alpha_i) = n_{hi}$, for $i = 1, 2, 3$, and $\rho(\alpha_o) = n_o$.

The extraction of \mathcal{R}_j is driven by a (hyper-parameter) *relation characterisation* $c_j : \mathcal{I} \rightarrow \{\text{true}, \text{false}\}$ for *relation type* t_j , with $j \in \{1, \dots, m\}$. For illustration, in Figure 1ii, dialectical relations of types support (+) and attack (-) may be defined by relation characterisations c_+ and c_- such that:²

- $c_+(n_1, n_2)$ is true iff $(n_1, n_2) \in \mathcal{I}$ and, for a_1 given by n_1 ’s activation and w_{12} the connection weight between n_1

²With an abuse of notation, we write $c_j(a, b)$ instead of $c_j((a, b))$, for any j .

and n_2 in \mathcal{N} , it holds that $w_{12}a_1 > 0$;

- $c_-(n_1, n_2)$ is true iff $(n_1, n_2) \in \mathcal{I}$ and, for a_1 and w_{12} as earlier, it holds that $w_{12}a_1 < 0$.

Thus, influences between nodes become dialectical relations of support (or attack) between the arguments representing them if the product of the activation of the “influencing” node and the weight of the connection with the “influenced” node (in the trained, underlying \mathcal{N}) is positive (or negative, resp.). Then, in the *extracted GAF*, an argument representing node n_1 supports an argument representing node n_2 iff $c_+(n_1, n_2) = \text{true}$ (similarly for attack and c_-). Note that we call the relation characterised by c_+ ‘support’ (and by c_- ‘attack’) as it is defined in terms of agreement (disagreement, resp.) between nodes and thus carries positive (negative, resp.) influence; the resulting relations are thus dialectical.

In this paper, we require that the choices allow to extract GAFs which (when seen as graphs with edges of m kinds) are trees with the output’s argument at the root (as in Figure 1ii). Formally:

Definition 2 Let hyper-parameters ρ, t_1, \dots, t_m and c_1, \dots, c_m be given. Then the extracted GAF $\langle \mathcal{A}, \mathcal{R}_1, \dots, \mathcal{R}_m \rangle$ is such that:

- $\mathcal{A} = \mathcal{A}_1 \cup \dots \cup \mathcal{A}_k$ where \mathcal{A}_i is the set of arguments representing the nodes at stratum N_i ;
- $\mathcal{A}_k = \{\alpha_o\}$ such that $\rho(\alpha_o) = n_o$;
- $\forall i \in \{2, \dots, k\}, \forall \alpha_h \in \mathcal{A}_i$ and $\forall n_g \in N_{i-1}$:
 $\exists \alpha_g \in \mathcal{A}_{i-1}$ such that $\rho(\alpha_g) = n_g$ iff
 $\exists (n_g, n_h) \in \mathcal{I}, \exists l \in \{1, \dots, m\}$ such that $c_l(n_g, n_h) = \text{true}$;
also, $(\alpha_g, \alpha_h) \in \mathcal{R}_l$, for $n_h = \rho(\alpha_h)$;
- $\forall (\alpha_p, \alpha_q), (\alpha_r, \alpha_s) \in \mathcal{R}_1, \dots, \mathcal{R}_m$ if $\rho(\alpha_p) = \rho(\alpha_r)$ and $\rho(\alpha_q) \neq \rho(\alpha_s)$ then $\alpha_p \neq \alpha_r$.

Intuitively arguments represent nodes and are partitioned so as to mirror the strata (first bullet); the single argument from the last stratum represents the output node (second bullet); nodes in (a stratum in) the influence graph are represented by arguments in the GAF iff they influence nodes (in the next stratum) represented by arguments themselves (because ultimately they lead to influences towards the output node) that contribute to one of the dialectical relations third bullet); a node influencing several nodes may need to correspond to several arguments, one for each influence that makes it into the dialectical relations (last bullet); for illustration, in Figure 1, two arguments α_{11} and α_{12} represent n_{x1} to distinguish between its influences on n_{h1} and n_{h2} .

Note that, by Definition 2, nodes which are not connected by influences do not contribute to dialectical relations in the GAF and nodes dialectically disconnected from the output node are not represented as arguments in the GAF. This secures the “relevance” of arguments in explanations drawn from the GAF. Note also that, given ρ , relation types and characterisations, there is a single extracted GAF according to Definition 2, whose depth reflects the depth of the influence graph from the first step.

Step 2 requires two final choices (of hyper-parameters), strongly coupled with the choice of relation types and char-

acterisations, and amounting to (*dialectical strength* (for arguments in the extracted GAF) and *dialectical properties* (see Section 2) for the chosen strength, guiding and regulating its choice to give rise to dialectically meaningful extracted GAFs. The notion of strength $\sigma : \mathcal{A} \rightarrow \mathbb{R}$ amounts to a quantitative measure derived from \mathcal{N} and giving dialectical meaning to the arguments in \mathcal{A} in the context of the chosen dialectical relations. In the running example, we can use activations to define σ too, by setting, for any $\alpha \in \mathcal{A}$, $\sigma(\alpha) = a$ with a the modulus of the activation of $\rho(\alpha)$ in \mathcal{N} .³

The choice of dialectical properties Π determine how “natural” the DAX obtained at Step 3 will be. A natural candidate

<i>Dialectical Monotonicity</i>	$\forall \alpha, \beta \in \mathcal{A}:$ $\mathcal{R}^-(\alpha) < \mathcal{R}^-(\beta) \wedge \mathcal{R}^+(\alpha) = \mathcal{R}^+(\beta) \rightarrow \sigma(\alpha) > \sigma(\beta);$ $\mathcal{R}^-(\alpha) = \mathcal{R}^-(\beta) \wedge \mathcal{R}^+(\alpha) < \mathcal{R}^+(\beta) \rightarrow \sigma(\alpha) < \sigma(\beta);$ $\mathcal{R}^-(\alpha) = \mathcal{R}^-(\beta) \wedge \mathcal{R}^+(\alpha) = \mathcal{R}^+(\beta) \rightarrow \sigma(\alpha) = \sigma(\beta).$
<i>Additive Monotonicity</i>	$\forall \alpha \in \mathcal{A}:$ $\sigma(\alpha) = \sum_{\beta \in \mathcal{R}^+(\alpha)} \sigma(\beta) - \sum_{\beta \in \mathcal{R}^-(\alpha)} \sigma(\beta).$

Table 1: Some dialectical properties for σ when using BAFs $\langle \mathcal{A}, \mathcal{R}^-, \mathcal{R}^+ \rangle$. We adopt notations as follows. (i) $\forall \alpha \in \mathcal{A}$ and $\mathcal{R}_i \in \{\mathcal{R}^-, \mathcal{R}^+\}$: $\mathcal{R}_i(\alpha) = \{\beta | (\beta, \alpha) \in \mathcal{R}_i\}$. (ii) $\forall A_1, A_2 \subseteq \mathcal{A}$: $A_1 \leq A_2$ iff \exists injective mapping $m : A_1 \mapsto A_2$ such that $\forall \alpha \in A_1$, $\sigma(\alpha) \leq \sigma(m(\alpha))$; $A_1 < A_2$ iff $A_1 \leq A_2 \wedge A_2 \not\leq A_1$; $A_1 = A_2$ iff $A_1 \leq A_2 \wedge A_2 \leq A_1$.

for inclusion in Π is *dialectical monotonicity* (see formalisation in Table 1 for BAFs, adapted from [Baroni *et al.*, 2018]), intuitively requiring that attacks weaken arguments and supports strengthen arguments. Another is *additive monotonicity* (see formalisation in Table 1, again for BAFs), requiring that an argument’s strength amounts to the sum of the strengths of its supporting arguments and the negations of the strengths of its attacking arguments.

Definition 3 Let $G = \langle \mathcal{A}, \mathcal{R}_1, \dots, \mathcal{R}_m \rangle$ be the extracted GAF given choices ρ, t_1, \dots, t_m and c_1, \dots, c_m . Let σ and Π be given. Then, G is Π -compliant under σ iff σ satisfies Π in G .

In the running example, with $\sigma(\alpha)$ given by the modulus of $\rho(\alpha)$ ’s activation dialectical monotonicity equates to the requirement that increasing the magnitude of a neuron’s activation results in a decrease (an increase) in magnitude of the activation of any neuron it attacks (supports, resp.) – and it is thus desirable for explanation of outputs in terms of attacks and supports. The BAF in the running example is dialectical monotonicity-compliant with some activation functions, e.g., it holds if *tanh* is used since for a given connection with weight w from activation a_1 towards a *tanh* activation a_2 , increasing (decreasing) wa_1 increases (decreases, resp.) a_2 . However, the BAF is not additive monotonicity-compliant, given that σ disregards connection weights in \mathcal{N} .

Several concrete choices (for hyper-parameters) may be possible and natural at Step 2, depending on the setting of deployment, the underlying NN and the choice of (hyper-parameter) N at Step 1, as we will see in Section 4. Note

³When strata are drawn from non-adjacent layers in \mathcal{N} (see Section 4), measures of strength/relation characterisations other than using activations will be needed.

that the choices of Π and σ are crucial to obtain dialectically meaningful DAXs at Step 3 (from extracted dialectical property-compliant GAFs under the chosen strength).

Step 3: from (dialectically compliant) GAFs to DAXs. This amounts to extracting, from the GAF and notion of strength from Step 2, a suitable DAX for the intended users. GAFs per se will typically not be suitable, firstly because their size may be (cognitively) prohibitive to users (as we shall see in Section 4), but also because, even when of manageable size, their outlook may not suit users’ requirements for the settings of deployment of explanations. The choice of DAX’s *format*, amounting to how much of the GAF from Step 2 to show users in which way, is determined by hyper-parameter ϕ , which, while guaranteeing that DAXs retain an argumentative outlook, takes into account the users’ needs. In our running example, Figure 1iii, ϕ selects only the “strongest” (according to σ) attackers and supporters in the GAF and delivers a *conversational* DAX.

Note that the selection of just some arguments (and dialectical relations involving them) matches other explanation methods, e.g., LIME, where only some features may be included to ensure that explanations are comprehensible to users. Also, conversational explanations (as in Figure 1iii) are advocated by several, e.g., in [Balog *et al.*, 2019]. For our instances in Section 4 we will explore, as part of ϕ , (interactive) graphical DAXs (e.g., as in Figure 4, discussed later).

Finally, users at the receiving end of explanations may also require appropriate *interpretations* of arguments and dialectical relations, returned by a suitably defined mapping χ (left unspecified in Figure 1iii, see Section 4 for some examples in our chosen instances). The definition of χ may benefit from work on explanation-as-visualisation (e.g., as in [Olah *et al.*, 2017; Bau *et al.*, 2017] for images). However, for DAXs, this interpretation only plays a role in the last step, on top of the GAF obtained from the first two.

4 Deploying the DAX framework

We show how to deploy the DAX framework with three specific neural architectures for prediction, trained on datasets/tasks as indicated. We give details for the first, and sketch the rest (further details can be found in Appendix A), focusing instead on motivating the underpinning choices for the hyper-parameters.

DAXs for CNNs for Text Classification. We targeted the CNN architecture in [Kim, 2014] with an input layer of 150 words followed by: an embeddings layer (6B GloVe embeddings of size 300); a hidden layer of 20 1D ReLU convolutional filters of which 10 of filter size 3, 5 of size 2 and 5 of size 4, followed by a max pooling layer; and finally a dense softmax layer. We trained this architecture with two datasets: a pre-processed version of AG-News [Gulli, 2005] (without HTML characters and punctuation) and IMDB [Maas *et al.*, 2011], in both cases tokenizing sentences using the spaCy tokenizer. In the remainder of this section we assume as given \mathcal{N} for either dataset.

Step 1. We chose hyper-parameter N with 3 strata: N_1 with nodes corresponding to the input words ($|N_1| = 150$), N_2 with nodes corresponding to the neurons of the max-pooling

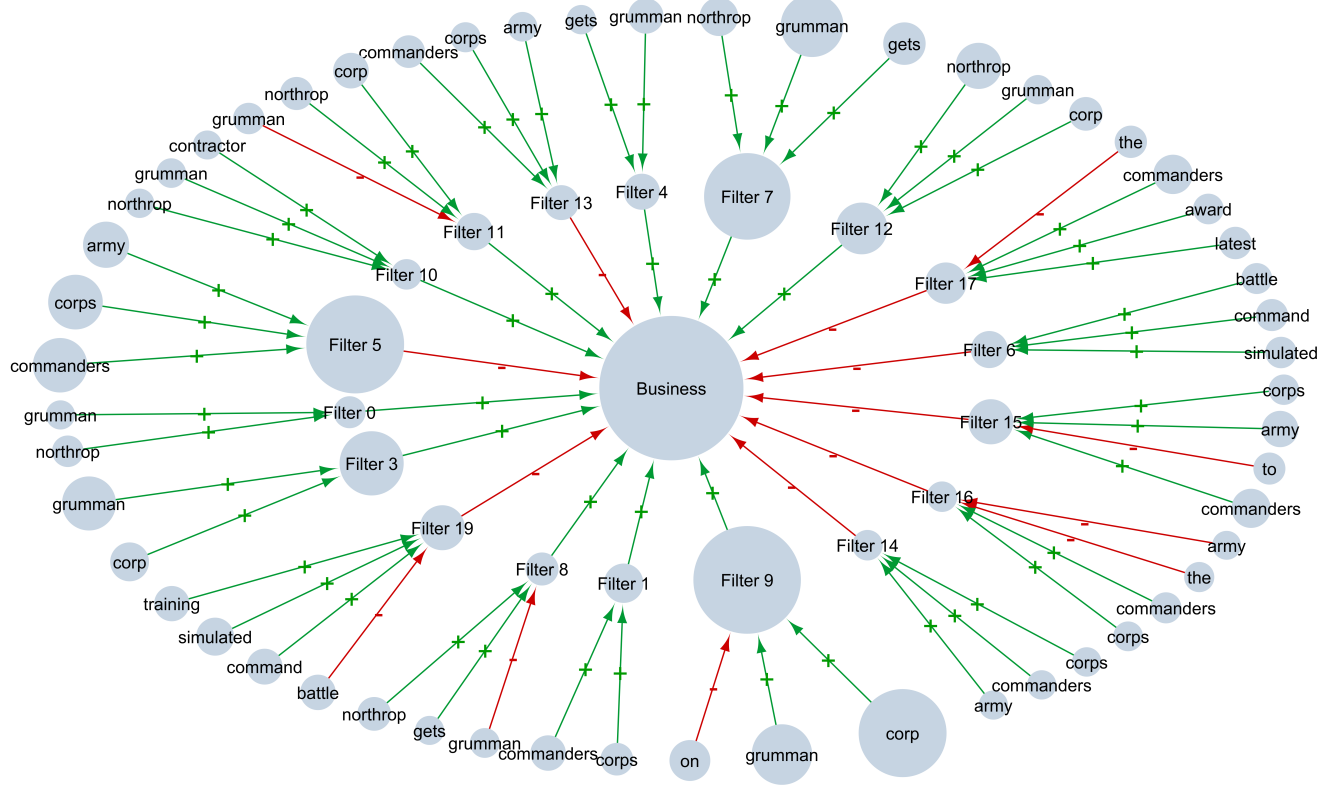


Figure 3: BAF from which the DAX for text CNN in Figure 4 is drawn. For each argument α , size corresponds to strength $\sigma(\alpha)$ and label corresponds to mapping to node $\rho(\alpha)$. Green (+) and red (-) arrows indicate, resp., support and attack.

layer ($|N_2| = 20$) and $N_3 = \{n_o\}$ where n_o is the neuron of the most probable class. Influences were then obtained as per Definition 1. Thus, the resulting influence graph mirrors closely the structure of the underlying \mathcal{N} .

Step 2. We chose to extract a BAF $\langle \mathcal{A}, \mathcal{R}^-, \mathcal{R}^+ \rangle$ with dialectical relations \mathcal{R}^- and \mathcal{R}^+ of types attack (i.e., negative influence) and support (i.e., positive influence, resp.), to show evidence and counter-evidence, resp., for predictions. An example such BAF (for a given input-output pair, with \mathcal{N} trained on AG-News) is shown in Figure 3. \mathcal{A} is divided in 3 disjoint sets, matching the strata: $\mathcal{A}_3 = \{\alpha_o\}$, with α_o the output argument; \mathcal{A}_2 is the set of all intermediate arguments α_j representing filters n_j in N_2 ; and \mathcal{A}_1 is the set of all input arguments α_{ij} , each representing a word n_i in N_1 that influences the filter n_j in N_2 . The mapping from arguments to nodes is thus defined, trivially, as $\rho(\alpha) = n_i \in N_1$ if $\alpha = \alpha_{ij} \in \mathcal{A}_1$, $\rho(\alpha) = n_j \in N_2$ if $\alpha = \alpha_j \in \mathcal{A}_2$ and $\rho(\alpha) = n_o$ if $\alpha = \alpha_o \in \mathcal{A}_3$. Even though in this DAX instantiation we chose to use the same types as in the toy illustration in Section 3, here we based the relation characterisations c_+ , c_- on LRP-0 [Bach *et al.*, 2015]. Formally, for $R(j, i)$ the LRP-0 relevance back-propagated from n_j back to n_i :⁴ $c_-(n_i, n_j) = \text{true}$ iff $R(j, i) < 0$ and $c_+(n_i, n_j) = \text{true}$ iff $R(j, i) > 0$. We also defined the di-

ialectical strength σ in terms of LRP-0: for a_p the activation of neuron n_p , $\sigma(\alpha) = a_o$ if $\alpha = \alpha_o \in \mathcal{A}_3$, $\sigma(\alpha) = |R(o, j)|$ if $\alpha = \alpha_j \in \mathcal{A}_2$ and $\sigma(\alpha) = |R(j, i)| \cdot \frac{R(o, j)}{a_j}$ if $\alpha = \alpha_{ij} \in \mathcal{A}_1$. We chose LRP because this is a robust, efficiently computable interpretability method. Also, we were driven by compliance with *dialectical monotonicity* and *additive monotonicity* from Table 1. These properties lead to BAFs from which DAXs aligning with human judgement can be drawn, as we will show in Section 6.

Step 3. The BAFs may be quite large (e.g., the one in Figure 3 includes 73 arguments). Also, their arguments (and the ones representing filters in particular), are unlikely to appeal to users (the intermediate ones are basically “black-boxes”). We chose to generate DAXs with only the top 3 supporters and attackers and in *graphical, interactive* format (ϕ), as shown in Figure 4 (for the same setting as in Figure 3, but limited to 4 arguments for space constraints). The interactive format of this DAX allows users to focus on particular parts (by clicking): this is especially useful to help users control the amount of information they receive.

The DAXs in this instance have 3 levels, aligning with the BAFs. Since convolutional filters/intermediate arguments are not intrinsically human-comprehensible, we opted (in the choice of mapping χ) to pair them with word clouds showing n-grams from input texts in samples in the training set that activate the most the corresponding filter, with the n-

⁴If n_i and/or n_j are groups of neurons then $R(j, i)$ is the sum of the relevances back-propagated from every neuron in n_j to every neuron in n_i .

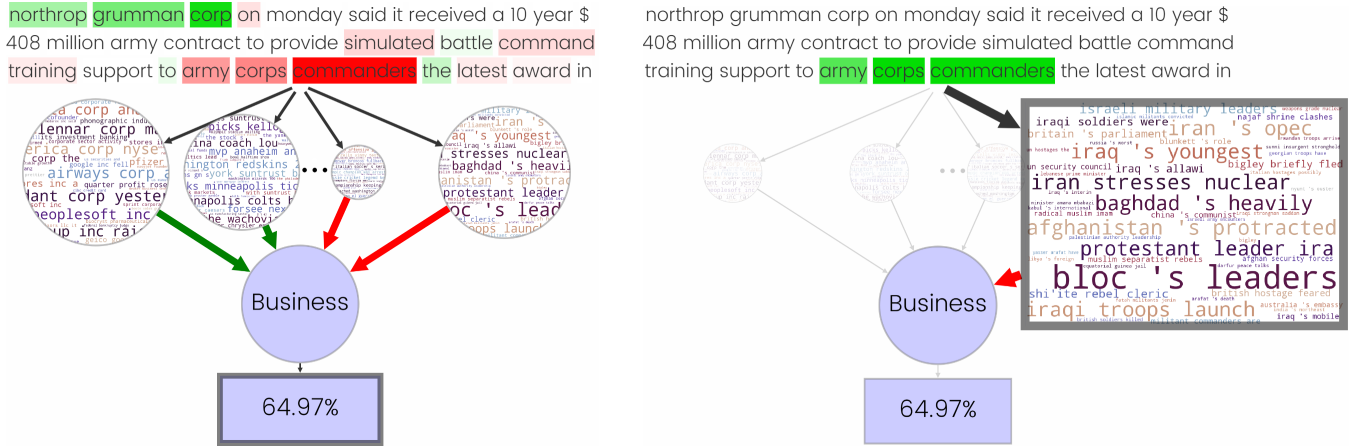


Figure 4: (Left) Graphical DAX for the (correct) output class “Business” (determined with 64.97% probability) by the CNN for text classification with AG-News, for the input article from AG-News at the top. (Right) The view of the DAX after clicking on the rightmost argument/word cloud. Arguments are visualised (by χ) as follows: *input words* with highlighting of a word given, on the left, by the sum of the (dialectical) strengths of all arguments representing that word and, on the right, by its corresponding argument’s dialectical strength; *convolutional filters/word clouds* with sizes the corresponding arguments’ strengths; and the most probable *class* and its probability. The green/red colours indicate, resp., support/attack (used on edges/relations from intermediate to output arguments, and on words from input to intermediate arguments).

grams’ size reflecting the number of activating samples, as in [Lertvittayakumjorn *et al.*, 2020]. We also chose to visualise attacks and supports from the intermediate arguments with red and green (resp.) arrows, and the attacks and supports from the input to the intermediate arguments (word clouds) differently in the static and interactive presentation of DAXs. In particular, when the word clouds are selected during interactions with the user, as in Figure 4, right (resulting from a user clicking on a word cloud, leading to this being magnified and the single words supporting or attacking it being highlighted), attacks and supports are arrows originating from red and green (resp.) words. Instead, when DAXs are shown in their initial, static form (as in Figure 4, left) the information about attacks and supports from input arguments (words) is reflected in the colours and intensity of the words, so that green and red represents words that overall support or attack the prediction, resp., and intensity the magnitude of their contribution.

DAXs for CNNs for Image Classification. To assess DAX’s applicability to deeper NNs, we considered a version of VGG16 [Simonyan and Zisserman, 2015] pre-trained on ImageNet [Deng *et al.*, 2009], with 1000 classes, 5 blocks of convolutional layers, a max pooling and 3 fully connected layers.

In Step 1, to avoid overwhelming users with information, we chose to ‘promote’ only 3 of the NN’s layers to strata: an input stratum N_1 whose nodes correspond to pixels in input images (combining 3 neurons each, for the pixels’ 3 RGB channels), an intermediate stratum N_2 whose nodes correspond to filters in the last convolutional layer (with each node a collection of 14x14 neurons) and an output stratum $N_3 = \{n_o\}$ with n_o the (single) neuron of the most probable (output) class. Overall, this gives $|N| = 224 \cdot 224 + 512 + 1$. We chose filters as members of N_2 because they are known

to naturally correspond to “concepts” amenable to intuitive visualisation based on activation maximization [Olah *et al.*, 2017; Kotikalapudi, 2017] by χ in Step 3.

In Step 2 we chose a GAF with a single relation of support (thus the GAF is a SAF, see Section 2), and used Grad-CAM weighted forward activation maps [Selvaraju *et al.*, 2020] to define relation characterisations and dialectical strength. We chose to exclude attack for simplicity, and because it does not naturally play a role in ImageNet. The choice of Grad-CAM, rather than LRP, is in line with the focus on support, given that it identifies features *positively* influencing predicted classes. To define relation characterisation and strength, we applied Grad-CAM not only to the “target concepts”, i.e., the classes, but also to the intermediate convolutional nodes/arguments. These choices give compliance with *dialectical monotonicity* and *additive monotonicity* properties (amounting, for SAFs, to removing all terms involving attack in the formulations in Table 1).

Finally, at Step 3, we may choose a variety of formats, including a similar format as for the text-CNN (see Appendix A), with (a suitable selection of) intermediate arguments visualised (by χ) using activation maximisation, as discussed earlier.

DAXs for FFNNs with tabular data. As third instance, we focused on NNs for tabular data, for which the identification of suitable explanation can be challenging [Le *et al.*, 2020]. Specifically, we deployed an FFNN for classification with the (categorical) COMPAS dataset [ProPublica, 2016], understanding *two_year_recid* as binary prediction (see Appendix A for details). The FFNN has 3 layers: an input layer that takes the one-hot encoding of the inputs, a dense hidden layer of size 8 with *tanh* activation followed by *ReLU* and an output layer with *sigmoid* activation.

In Step 1, we chose to keep as much as possible of the (small)

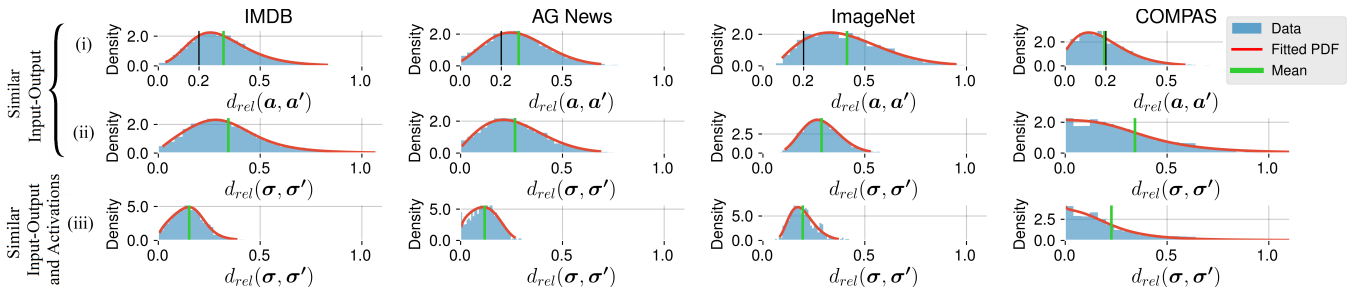


Figure 5: Distributions of difference of (i) intermediate strata activations and (ii) intermediate arguments’ strengths, for given and *similar* input-output pairs, and (iii) of strengths of *similar* input-output pairs that also have *similar* activations. Here, for \mathbf{x} and \mathbf{x}' two vectors (of activations or strengths), the relative difference between \mathbf{x} and \mathbf{x}' is $d_{rel}(\mathbf{x}, \mathbf{x}') = \frac{2 \cdot ||\mathbf{x}' - \mathbf{x}||_1}{||\mathbf{x}'||_1 + ||\mathbf{x}||_1}$.

NN; thus the first two layers coincide with the respective strata and the last layer amounts to the most probable class node n_o from the last stratum, giving $|N| = 58 + 8 + 1$.

In *Step 2*, we opted for a form of GAF able to unearth evidence and counter-evidence (in the spirit of the text-CNN), while being able to represent *counter-factual*, useful to identify possible biases in N (often a concern with classifiers for COMPAS). The GAF is a TAF $\langle \mathcal{A}, \mathcal{R}^-, \mathcal{R}^+, \mathcal{R}^{+!} \rangle$ with dialectical relations, resp., of attack, support and *critical support*, drawn from essential positive influences removing which would lead to different predictions. We chose to define strength and relation characterisations in terms of activations (as for the toy illustration in Section 3), as this reflects well our desired counter-factual behaviour of $\mathcal{R}^{+!}$: intuitively, c_+ defines a critical support between arguments representing n_i and n_j iff deactivating n_i causes the deactivation of n_j (i.e., n_i ’s positive contribution is essential for n_j ’s activation). These choices lead to compliance with the dialectical property of *counter-factual*, requiring that the removal of critical support from an argument to another with positive dialectical strength will result in the strength of the latter becoming zero or lower.

In *Step 3* we may again choose, amongst others, a graphical, interactive DAX with 3 levels reflecting the strata/argument structure. No matter the format, we need to take the (non-trivial) decision on how to visualise (via χ) the intermediate arguments/hidden neurons and the dialectical relations so they are human-comprehensible. For example, we could choose pie charts showing intermediate arguments and their incoming attacks, supports and critical supports from input arguments (see Appendix A).

5 Empirical Evaluation

We consider, for the DAX instances in Section 4, two dimensions: *computational cost* (standard in the literature [Sokol and Flach, 2020]) and a novel *deep-fidelity*, tailored to deep explanations such as DAXs.

Computational cost. Firstly note that, although the choice of $\langle N, \mathcal{I} \rangle$ is tailored to explaining $f(x) = o$, for specific input-output pairs (x, o) , the choice of candidate nodes in N from the hidden layers can be made a-priori, independently of any pair. Also, the skeleton underpinning the construction of DAXs relies exclusively on the given NN, prior to training.

Thus, there is a single one-off cost for constructing DAXs that can be shared across pairs. Secondly, the time complexity to calculate DAXs is relatively small: there is a one time cost for χ , but the cost to generate a single DAX is comparable to the cost of a single prediction and single (for the FFNN instance) or multiple (for LRP and Grad-CAM in the CNN instances) back-propagation steps. The time cost depends *linearly* on the size of N . Formally, for the text-CNNs, given the time cost for a prediction c_f (1.7 ± 0.4 ms, in our experiments) and the cost to back-propagate the output to the inputs c_b (50.2 ± 11.0 ms, in our experiments) while we let c be any other (constant or negligible) computational cost, the (one-time) generation of the word clouds using n_S training samples (we used 1000 for Figure 4) has time complexity: $O(n_S \cdot (c_f + c_b) \cdot |N_2| + c)$. The time complexity to generate a single DAX is instead: $O(c_f + c_b \cdot |N_2| + c)$. Details for the other instances are in Appendix A. Here, note that the setup took up to 2:35 hours for the VGG16 instance while the time to generate a single DAX ranged from under 1ms (for the FFNN) to 4.35s (for VGG16).

Deep-fidelity. Fidelity of generated explanations to the model being explained is widely considered an important property for XAI methods (e.g., see [Sokol and Flach, 2020]), but existing notions of fidelity are mostly tailored to the dominant view of “flat” explanations, for outputs given the inputs, and their underpinning assumptions are unsuitable for deep explanations. As an example, [Jacovi and Goldberg, 2020] poses that explanations for similar inputs for which the underlying model computes similar outputs should in turn be similar. This disregards the possibility that the model computes these outputs in completely different manners. Indeed, we assessed this empirically for our three settings, showing that it does not hold. We defined similarity as follows. For text classification, we generated similar input pairs back-translating from French [Ribeiro *et al.*, 2018] using Google Translate; for images we paired each image with a noisy counterpart (Gaussian noise of $std = 10$); for tabular data we paired each sample with another sample with one categorical feature changed. In all settings, we considered outputs to be similar when the predicted probability changed less than 5%. Our experiments show that activations of the intermediate strata could differ considerably when inputs and outputs are similar, with an average relative difference ranging between

19.2% and 41.3%, as shown in Fig. 5i. Our DAXs are able to match this inner diversity, as shown in Fig. 5ii, where we note how also the intermediate arguments’ strengths follow this behaviour of the model. Our novel notion of *deep-fidelity*, suitable for evaluating DAXs (and deep explanations in general), sanctions that “*deep explanations for similar inputs for which the underlying model similarly computes similar outputs should in turn be similar*”. In order to assess this property, we added an additional constraint for two samples to be regarded as similar, requiring that also the intermediate strata activations must be similar. Experimentally, we considered activations to be similar if their average relative distance was less than 20% (see Fig. 5 caption for the formal definition). As shown in Fig. 5iii, our explanations consistently reflect this constraint, showing a reduction of the average difference between the strengths of the intermediate strata arguments of 32.2%-55.8%.

6 Experimental Results

We conducted experiments with 72 participants on Amazon Mechanical Turk, to assess: (A) whether DAXs are comprehensible; (B) whether DAXs align with human judgement and (C) how desirable DAXs are when compared to other explanation methods with an argumentative spirit. We focused on text classification with AG-News. We chose this setting because topic classification (AG-News) is multiclass (4 classes) – thus more complex than (binary) sentiment analysis (IMDB); also, it requires no domain expertise (unlike COMPAS) and has not been widely studied (unlike ImageNet). The participants were non-expert (see Appendix C), showing that DAX’s target audience may be broad.

In the experiments, we used only samples in the test set predicted with high confidence (i.e., with probability over 0.95); we did so as, for samples predicted with lower confidence, if the explanations are implausible to users, we cannot know whether this is due to the poor underlying model or the explanations themselves. To obtain interpretations (by χ) of intermediate arguments in DAXs we used word clouds (see Section 4) generated from 1000 random training samples. We considered a *filter* to be *strongly activated* (by the input-output pair being explained) if its activation was greater than the 90th percentile of the activations of the 1000 training samples, and *weakly activated* if its activation was lower than the 1st percentile. We considered a *class* to be *strongly supported* by an intermediate argument if the latter’s strength ranked in the top 20% of the arguments supporting the class.

(A) Comprehensibility. The following research questions aim to ensure that humans can understand the interplay between intermediate arguments (i.e., word clouds) and other arguments (i.e., input words, output classes). **RQ1:** “*Can humans understand the roles of individual intermediate arguments towards the output by examining their word clouds?*” To answer RQ1, we showed participants a word cloud and asked them to select the class they best associated with it. **Results:** Over 97% ($\pm 0.3\%$) of answers picked a class strongly supported by the presented argument, confirming human understanding. **RQ2:** “*Can humans understand the patterns of intermediate arguments by examining their word clouds?*” To

answer RQ2, we asked participants to select from 4 n-grams that which best matched the pattern in the word cloud of a strongly activated filter. The 4 n-grams were extracted from input texts correctly predicted with high confidence by the CNN, and the CNN’s best-match was selected by the max pooling, while the others weakly activated the filter. **Results:** Participants answered correctly in 65.5% ($\pm 1\%$) of the cases. We posit this result as positive as random guesses can lead to 25% correct answers and the task is not trivial without NLP experience, as was the case for 96% of participants (see Appendix C). **RQ3:** “*Can humans understand the NN from the dialectical relations originating from the intermediate arguments only, without the input?*” To answer RQ3, we first showed only the strongest supporter and attacker of the predicted class, and then added the next strongest supporter and attacker, and so on until 4 of each were shown. At each step we asked the participants to select the class they would predict. **Results:** The strongest supporter and attacker sufficed for participants to correctly classify samples in over 80% of the cases. Thus, even partial information about the intermediate arguments gives strong insight into the model.

(B) Alignment with Human Judgement. We assessed whether DAXs (especially support) align with human judgement when the CNN confidently and correctly predicts a certain class. **RQ4:** “*Do supports between intermediate arguments and predicted class in DAXs align with human judgement?*” To answer RQ4, we showed n-grams extracted from input texts correctly predicted with high confidence and selected by a strongly activated filter (but without showing the word cloud) and asked participants to select the class this n-gram is best associated with. **Results:** In over 96% ($\pm 0.4\%$) of the answers, participants selected a class that the n-gram strongly supports. **RQ5:** “*Do supports between individual words and intermediate arguments in DAXs align with human judgement?*” To answer RQ5, we showed n-grams extracted from input texts correctly predicted with high confidence of a strongly activated filter together with its word cloud and asked participants to select a word (in the n-grams) fitting best with phrases in the word cloud amongst 2 words: the strongest supporter and attacker of the intermediate argument representing the filter. **Results:** In 85% ($\pm 0.7\%$) of the answers to RQ5, participants chose the correct answer. This assured us that our notion of support aligns with human judgement.

(C) User Acceptance. To assess whether *deep* explanations, in the form of DAXs, are amenable to humans in comparison with “flat” explanations, we chose to compare DAXs and existing methods with a somewhat similar argumentative spirit as the BAF-based DAXs we have deployed for text classification (in particular, we chose the popular LIME and SHAP forms of explanation, presented in their standard formats within the available LIME and SHAP libraries). To compare DAXs and LIME/SHAP in terms of user acceptance, we asked participants to rate explanations according to (desirable) criteria: (1) ease of understanding; (2) ability to provide insight into the internal functioning of the CNN; (3) capability of inspiring trust in users. We showed each participant an example consisting of the input text, the predicted class with its confidence, and three explanations (varying the order in

different experiments): a baseline (a graph showing the probability of each class), a DAX, and the explanation computed by LIME or SHAP. **Results:** (See Figure 6) As expected, DAXs give more insight on the CNN internal working when compared with LIME ($p < 0.004$) and SHAP ($p < 0.006$). Finally, DAXs significantly inspire more trust when compared with SHAP ($p < 0.002$) although the increase in trust is not significant when compared with LIME ($p = 0.32$). We posit that this is due to the lack of expertise of participants (less than 12% of participants stated that they had expertise in machine learning, NNs or deep learning). We also posit, and leave to future studies, that these benefits may be more significant with expert participants.

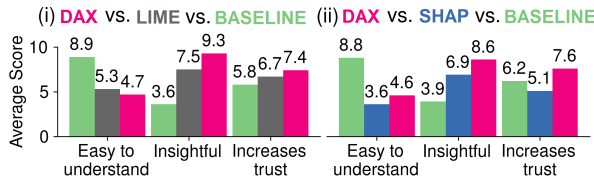


Figure 6: Participants’ average scores when comparing DAX with a baseline and LIME (i) or SHAP (ii). Scores were converted from a discrete scale (“No”, “Somewhat”, “Yes”) to numerical scores (0,5,10) for ease of comprehension.

7 Conclusions

We presented novel Deep Argumentative Explanations (DAXs), resulting from a marriage between symbolic AI (in the form of computational argumentation) and neural approaches, and leveraging on the amenability of argumentation for explanation to humans and on several advances in the field of computational argumentation, as well as in interpretability and visualisation of NNs. DAXs can be used to cast light on the inner working of NNs beyond visualisation and are adaptable to fit a variety of explanatory settings. We also presented three DAX instances, amounting to novel stand-alone contributions per se that can be readily deployed in other tasks supported by the same neural architectures. We studied (existing and novel) empirical properties of our DAX instances, and conducted experiments, with lay participants, to show that DAXs can be desirable from the user perspective. Future work includes exploring further DAX instances, properties, and evaluation by expert users.

Acknowledgements

This research was funded in part by J.P. Morgan and by the Royal Academy of Engineering under the Research Chairs and Senior Research Fellowships scheme. Any views or opinions expressed herein are solely those of the authors listed, and may differ from the views and opinions expressed by J.P. Morgan or its affiliates. This material is not a product of the Research Department of J.P. Morgan Securities LLC. This material should not be construed as an individual recommendation for any particular client and is not intended as a recommendation of particular securities, financial instruments or strategies for a particular client. This material

does not constitute a solicitation or offer in any jurisdiction. We thank Kristijonas Cyras for helpful comments on earlier versions of this paper.

References

- [Aas *et al.*, 2019] Kjersti Aas, Martin Jullum, and Anders Løland. Explaining individual predictions when features are dependent: More accurate approximations to shapley values. *CoRR*, abs/1903.10464, 2019.
- [Alvarez-Melis and Jaakkola, 2018] David Alvarez-Melis and Tommi S. Jaakkola. Towards robust interpretability with self-explaining neural networks. In *NeurIPS*, pages 7786–7795, 2018.
- [Amgoud and Ben-Naim, 2016] Leila Amgoud and Jonathan Ben-Naim. Evaluation of arguments from support relations: Axioms and semantics. In *IJCAI*, pages 900–906, 2016.
- [Antaki and Leudar, 1992] Charles Antaki and Ivan Leudar. Explaining in conversation: Towards an argument model. *Euro. J. of Social Psychology*, 22:181–194, 1992.
- [Atkinson *et al.*, 2017] Katie Atkinson, Pietro Baroni, Massimiliano Giacomini, Anthony Hunter, Henry Prakken, Chris Reed, Guillermo Ricardo Simari, Matthias Thimm, and Serena Villata. Towards artif. argumentation. *AI Magazine*, 38(3):25–36, 2017.
- [Bach *et al.*, 2015] Sebastian Bach, Alexander Binder, Grégoire Montavon, Frederick Klauschen, Klaus-Robert Müller, and Wojciech Samek. On pixel-wise explanations for non-linear classifier decisions by lrp. *PLOS ONE*, 10(7):1–46, 07 2015.
- [Balog *et al.*, 2019] Krisztian Balog, Filip Radlinski, and Shushan Arakelyan. Transparent, scrutable and explainable user models for personalized recommendation. In *SIGIR*, pages 265–274, 2019.
- [Baroni *et al.*, 2018] Pietro Baroni, Antonio Rago, and Francesca Toni. How many properties do we need for gradual argumentation? In *AAAI*, 2018.
- [Bau *et al.*, 2017] David Bau, Bolei Zhou, Aditya Khosla, Aude Oliva, and Antonio Torralba. Network dissection: Quantifying interpretability of deep visual representations. In *CVPR*, pages 3319–3327, 2017.
- [Briguez *et al.*, 2014] Cristian E. Briguez, Maximiliano C. Budán, Cristhian A. D. Deagustini, Ana G. Maguitman, Marcela Capobianco, and Guillermo R. Simari. Argument-based mixed recommenders and their application to movie suggestion. *Expert Systems with Applications*, 41(14):6467–6482, 2014.
- [Cayrol and Lagasquie-Schiex, 2005] Claudette Cayrol and Marie-Christine Lagasquie-Schiex. On the acceptability of arguments in bipolar argumentation frameworks. In *ECSQARU*, pages 378–389, 2005.
- [Chen *et al.*, 2020] Hanjie Chen, Guangtao Zheng, and Yangfeng Ji. Generating hierarchical explanations on text classification via feature interaction detection. *CoRR*, abs/2004.02015, 2020.

- [Cocarascu *et al.*, 2020] Oana Cocarascu, Elena Cabrio, Serena Villata, and Francesca Toni. Dataset independent baselines for relation prediction in arg. mining. In *COMMA*, pages 45–52, 2020.
- [Deng *et al.*, 2009] Jia Deng, Wei Dong, Richard Socher, Li-Jia Li, Kai Li, and Fei-Fei Li. Imagenet: A large-scale hierarchical image database. In *CVPR*, pages 248–255, 2009.
- [Dung, 1995] Phan M. Dung. On the acceptability of arguments and its fundamental role in nonmonotonic reasoning, logic programming and n-person games. *Artif. Intel.*, 77(2):321 – 357, 1995.
- [Gabbay, 2016] Dov M. Gabbay. Logical foundations for bipolar and tripolar argumentation networks: preliminary results. *J. Log. Comput.*, 26(1):247–292, 2016.
- [Guidotti *et al.*, 2019] Riccardo Guidotti, Anna Monreale, Salvatore Ruggieri, Franco Turini, Fosca Giannotti, and Dino Pedreschi. A survey of methods for explaining black box models. *ACM Comput. Surv.*, 51(5):93:1–93:42, 2019.
- [Gulli, 2005] Antonio Gulli. AG-News Corpus, 2005.
- [Ignatiev *et al.*, 2019] Alexey Ignatiev, Nina Narodytska, and João Marques-Silva. On relating explanations and adversarial examples. In *NeurIPS*, pages 15857–15867, 2019.
- [Jacovi and Goldberg, 2020] Alon Jacovi and Yoav Goldberg. Towards faithfully interpretable NLP systems: How should we define and evaluate faithfulness? In *ACL*, pages 4198–4205, 2020.
- [Kim, 2014] Yoon Kim. Convolutional neural networks for sentence classification. In *EMNLP*, pages 1746–1751, 2014.
- [Kotikalapudi, 2017] Raghavendra Kotikalapudi. keras-vis, 2017. GitHub.
- [Kunkel *et al.*, 2019] Johannes Kunkel, Tim Donkers, Lisa Michael, Catalin-Mihai Barbu, and Jürgen Ziegler. Let me explain: Impact of personal and impersonal explanations on trust in recommender systems. In *CHI*, page 487, 2019.
- [Le *et al.*, 2020] Thai Le, Suhang Wang, and Dongwon Lee. GRACE: generating concise and informative contrastive sample to explain neural network model’s prediction. In *SIGKDD*, pages 238–248, 2020.
- [Lertvittayakumjorn *et al.*, 2020] Piyawat Lertvittayakumjorn, Lucia Specia, and Francesca Toni. FIND: human-in-the-loop debugging deep text classifiers. In *EMNLP*, pages 332–348, 2020.
- [Lippi and Torroni, 2016] Marco Lippi and Paolo Torroni. Argumentation mining: State of the art and emerging trends. *ACM Trans. Internet Techn.*, 16(2):10:1–10:25, 2016.
- [Lundberg and Lee, 2017] Scott M. Lundberg and Su-In Lee. A unified approach to interpreting model predictions. In *NeurIPS*, pages 4765–4774, 2017.
- [Maas *et al.*, 2011] Andrew L. Maas, Raymond E. Daly, Peter T. Pham, Dan Huang, Andrew Y. Ng, and Christopher Potts. Learning word vectors for sentiment analysis. In *ACL*, pages 142–150, 2011.
- [Miller, 2019] Tim Miller. Explanation in artificial intelligence: Insights from the social sciences. *Artif. Intel.*, 267:1–38, 2019.
- [Naveed *et al.*, 2018] Sidra Naveed, Tim Donkers, and Jürgen Ziegler. Argumentation-based explanations in recommender systems: Conceptual framework and empirical results. In *UMAP*, pages 293–298, 2018.
- [Olah *et al.*, 2017] Chris Olah, Alexander Mordvintsev, and Ludwig Schubert. Feature visualization. *Distill*, 2017.
- [Olah *et al.*, 2018] Chris Olah, Arvind Satyanarayan, Ian Johnson, Shan Carter, Ludwig Schubert, Katherine Ye, and Alexander Mordvintsev. The building blocks of interpretability. *Distill*, 2018.
- [ProRepublica, 2016] ProRepublica. COMPAS Recidivism Risk Score Data and Analysis, 2016.
- [Rader *et al.*, 2018] Emilee J. Rader, Kelley Cotter, and Janghee Cho. Explanations as mechanisms for supporting algorithmic transparency. In *CHI*, page 103, 2018.
- [Rago *et al.*, 2018] Antonio Rago, Oana Cocarascu, and Francesca Toni. Argumentation-based recommendations: Fantastic explanations and how to find them. In *IJCAI*, 2018.
- [Ribeiro *et al.*, 2016] Marco Túlio Ribeiro, Sameer Singh, and Carlos Guestrin. "why should I trust you?": Explaining the predictions of any classifier. In *SIGKDD*, pages 1135–1144, 2016.
- [Ribeiro *et al.*, 2018] Marco Túlio Ribeiro, Sameer Singh, and Carlos Guestrin. Semantically equivalent adversarial rules for debugging NLP models. In *ACL*, pages 856–865, 2018.
- [Selvaraju *et al.*, 2020] Ramprasaath R. Selvaraju, Michael Cogswell, Abhishek Das, Ramakrishna Vedantam, Devi Parikh, and Dhruv Batra. Grad-cam: Visual explanations from deep networks via gradient-based localization. *Int. J. Comput. Vis.*, 128(2), 2020.
- [Shih *et al.*, 2018] Andy Shih, Arthur Choi, and Adnan Darwiche. A symbolic approach to explaining bayesian network classifiers. In *IJCAI*, pages 5103–5111, 2018.
- [Simonyan and Zisserman, 2015] Karen Simonyan and Andrew Zisserman. Very deep convolutional networks for large-scale image recognition. In *ICLR*, 2015.
- [Sokol and Flach, 2020] Kacper Sokol and Peter A. Flach. Explainability fact sheets: a framework for systematic assessment of explainable approaches. In *FAT**, pages 56–67, 2020.
- [Wang and Nasconcelos, 2019] Pei Wang and Nuno Nasconcelos. Deliberative explanations: visualizing network insecurities. In *NeurIPS*, pages 1372–1383, 2019.

Appendices

A DAX Instances: Additional Details

For all models we used Keras with Adam optimizer and set random seeds of Python (`random`), NumPy and TensorFlow/Keras to 0.

CNN for text classification We trained the network in batches of 128 samples for a maximum of 100 epochs with an early stopping with patience 3. We split the IMDB dataset in training (20000 samples), validation (5000) and test (25000) sets, achieving accuracy of 81.81% on the test set. We split the AG-News dataset in training (96000 samples), validation (24000) and test (7600) sets, pre-processing to remove HTML characters, punctuation and lowering all text, achieving accuracy of 90.14% on the test set. The hyper-parameters of the text-CNNs were chosen after exploring: batch size $\in \{64, 128, 256, 512\}$; patience $\in \{3, 5\}$; dropout $\in \{0.0, 0.1, 0.2, 0.3, 0.5\}$; and several filters sizes sets.

CNN for Image Classification We used VGG-16 (pre-trained on ImageNet) as available in Keras. This has a top-1 accuracy of 71.3% and a top-5 accuracy of 90.1% on ImageNet validation set.

In Step 2, we chose to extract SAFs $\langle \mathcal{A}, \mathcal{R}^+ \rangle$ with \mathcal{A} divided in 3 disjoint sets, corresponding to the strata: $\mathcal{A}_3 = \{\alpha_o\}$, with α_o the *output argument*; \mathcal{A}_2 is the set of all *intermediate arguments* α_j representing convolutional filter n_j in the second stratum; \mathcal{A}_1 is the set of all the *input arguments* α_{xyj} representing a pixel n_{xy} in the input image influencing a convolutional filter n_j in the second stratum. Overall, this gives SAFs with as many as 1,472,224 arguments (as in the case of the SAF from which the DAX in Figure 7 is drawn). We defined the relation characterisation (for \mathcal{R}^+) and the dialectical strength σ in terms of the Grad-CAM weighted forward activation maps [Selvaraju *et al.*, 2020] of the last convolutional layer, as follows. Let G_j^o be the (Grad-CAM) weighted forward activation map of filter j (in the last convolutional layer) resized to the input size, and g_j^o the Grad-CAM neuron importance weight of filter j for class c in the last convolutional layer. Then

$$c_+(n, m) = \begin{cases} \text{true} & \text{if } n = n_j \wedge g_j^o > 0 \\ \text{true} & \text{if } n = n_{xy} \wedge m = n_j \wedge G_j^o(x, y) > 0 \\ \text{false} & \text{otherwise} \end{cases}$$

$$\sigma(\alpha) = \begin{cases} \sum_{j,x,y} G_j^o(x, y) & \text{if } \alpha = \alpha_o \in \mathcal{A}_2 \\ \sum_{x,y} G_j^o(x, y) & \text{if } \alpha = \alpha_j \in \mathcal{A}_1 \\ G_j^o(x, y) & \text{if } \alpha = \alpha_{xyj} \in \mathcal{A}_0 \end{cases}$$

In Step 3, we chose ϕ giving a graphical, interactive DAX where only 8 amongst the 512 intermediate arguments (filters) are shown to the user (these are the 8 arguments with highest strength). Figure 7 shows the DAX for an input image predicted by the model to be an electric guitar (with probability 80.23%) after clicking on the left-most argument (that seems associated with the visual concept of “guitar cords”). We chose χ for intermediate arguments so that

$$\chi(\alpha_j) = \arg \max_{A^j} (\mathcal{L}_{act}(A^j) + \beta_{LP}^j \cdot \mathcal{L}_{LP}(A^j) + \beta_{LP} \cdot \mathcal{L}_{TV}(A^j))$$

where \mathcal{L}_{act} , \mathcal{L}_{LP} and \mathcal{L}_{TV} are, resp., the activation, LP-norm

and total variation losses. To compute it we used Keras-vis with $\beta_{LP} = 10$. We ran the maximisation multiple times for filters for which the algorithm did not converge (by manual inspection) seeding each run with the output of the previous: we used first a jitter of 0.05 and 200 iterations, then of 0.02 and 500 iterations, then of 0.04 and 1000 iterations, then of 0.05 and 1500 iterations, then of 0.05 and 3000 iterations, and finally of 0.01 and 1000 iterations, after which all filters’ activation maximizations converged. In each run we first set β_{TV} to 0 and then re-run with $\beta_{TV} = 10$ to denoise the output.

Feed-forward NN with tabular data In COMPAS, we used `sex`, `age`, `race`, `juv_fel_count`, `juv_misd_count`, `juv_other_count`, `priors_count`, `is_recid`, `is_violent_recid`, `custody`, `charge_desc`, `charge_degree` as categorical input features, and `two_year_recid` as binary prediction. We removed all records with unknown value and transformed into categorical variables `custody`, `priors_count`, `juv_other_count`, `juv_fel_count` and `juv_misd_count`. We trained the network in batches of size 32 for a maximum of 10 epochs with early stopping with patience 5. We split the dataset in training (5213 samples) and test (1738 samples) sets. The trained (10 epochs) network has prediction accuracy of 70.2% on the test set. The low prediction accuracy did not affect our results since our goal was to *explain* the internal mechanism of the NN in making predictions (no matter how accurately). The hyper-parameters of the NN were chosen after exploring the following alternatives: hidden layer activation function $\in \{\tanh, \text{relu}, \tanh + \text{relu}\}$; batch size $\in \{4, 8, 16, 32, 64\}$.

In Step 1, N_1 ($|N_1| = 58$) with $n_f \in N_1$ corresponding to input neuron f , N_2 such that $n_j \in N_2$ is the node corresponding to the hidden neuron j after (tanh and) ReLU activation ($|N_2| = 8$), and $N_3 = \{n_o\}$ with n_o the most probable class node.

In Step 2, we chose to obtain TAFs $\langle \mathcal{A}, \mathcal{R}^-, \mathcal{R}^+, \mathcal{R}^{+!} \rangle$, as follows. \mathcal{A} consists of 3 disjoint sets: $\mathcal{A}_3 = \{\alpha_o\}$, where α_o is the *output argument*; \mathcal{A}_2 is the set of *intermediate arguments* α_j representing a node (hidden neuron) n_j in the second stratum; \mathcal{A}_1 is the set of *input arguments* α_{ij} representing an input node (neuron) n_i in the first stratum influencing a node n_j in the second stratum. Let a_x be the activation of neuron n_x and w_{xy} be the connection weight between n_x and neuron n_y . Then:

$$c_-(n_x, n_y) = \text{true} \quad \text{iff } w_{xy} a_x < 0$$

$$c_+(n_x, n_y) = \text{true} \quad \text{iff } w_{xy} a_x > 0$$

$$c_{+!}(n_x, n_y) = \text{true} \quad \text{iff } a_y > 0 \wedge a_y - w_{xy} a_x \leq 0$$

$$\sigma(\alpha) = \begin{cases} a_o & \text{if } \alpha = \alpha_o \in \mathcal{A}_2 \\ |w_{jo} \cdot a_j| & \text{if } \alpha = \alpha_j \in \mathcal{A}_1 \\ |w_{ij} \cdot w_{jo} \cdot a_i| & \text{if } \alpha = \alpha_{ij} \in \mathcal{A}_0 \end{cases}$$

Formally, $\langle \mathcal{A}, \mathcal{R}^-, \mathcal{R}^+, \mathcal{R}^{+!} \rangle$ is *counter-factuality-compliant* under σ iff for any $\alpha, \beta \in \mathcal{A}$, if $(\alpha, \beta) \in \mathcal{R}^{+!}$ then $\sigma(\beta) > 0$ and $\sigma(\beta) - \sigma(\alpha) \leq 0$.

The TAFs resulting from Step 2 are clearly not human-friendly. In Step 3, we can generate DAXs with 3 levels reflecting the strata structure of the same graphical, interactive format as for the other two instances. As for χ , we can visualise arguments as shown in Figure 9. This choice deals with the peculiarity of this FFNN in which input arguments/features

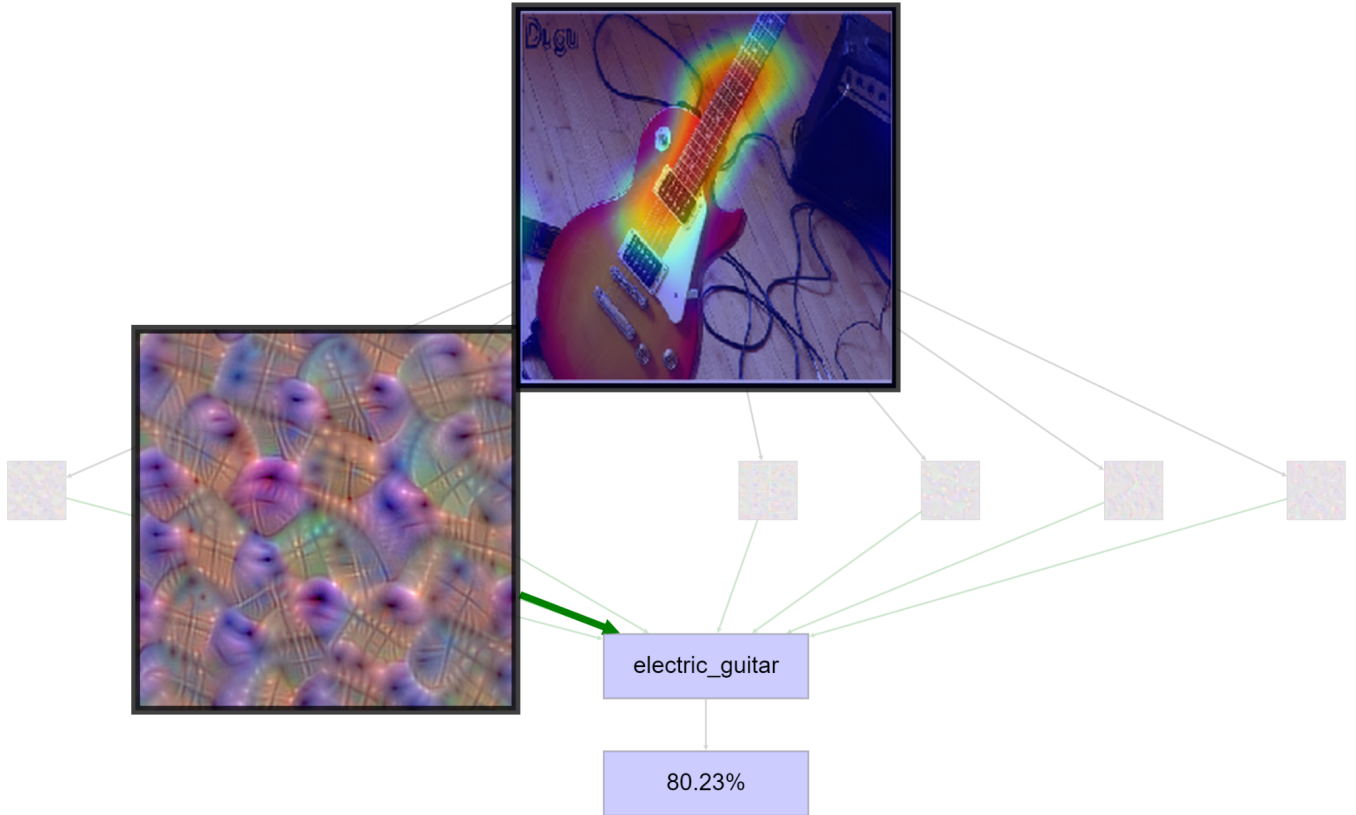


Figure 7: Graphical interactive DAX for image classification of an image from ImageNet. We use $\chi(\alpha)$ such that for argument α a pixel in the input image we use red for the strongest supporters (of the convolutional filter), then green, then blue (thus giving rise to a heatmap of the input image), and for argument α a filter we use the activation maximisation of that filter. The green colour of the arrows indicates support (from filters to output argument/prediction).

can only be 0 or 1 (because of the one-hot encoding) while (arguably) providing human-understandable readings of intermediate arguments/hidden neurons.

B Details of empirical evaluation

For the experiments in Section 5, we used 1) for the text-CNN instances, for both datasets, the test sets; 2) for the image-CNN, we downloaded a randomized sample of correctly predicted images from ImageNet; 3) for the FNN for COMPAS, the test set. To run all experiments, we used a Python 3.6 environment with numpy 1.18.1, pandas 1.0.3, Keras 2.2.4, TensorFlow 1.12, SpaCy 2.2.3, shap 0.31.0, Keras-vis 0.4.1, investigate 1.0.8 and lime 0.2.0.0 as software platform on a single Nvidia RTX 2080 Ti GPU with 11GB of memory on a machine with an Intel i9-9900X processor and 32GB of RAM.

Computational Costs (Image-CNN and FFNN). For the CNN for image classification, given the time cost for an iteration of the feature activation maximization algorithm c_g (39.1 ± 8.5 ms, in our experiments) while we let c be any other (constant or negligible) computational cost, the generation of the feature activation maximization maps (a one-time cost for χ) with n_I iteration (we used between 200 and 3000 to generate the Figure 7, depending on the filter convergence characteristics) has time complexity $O(c_g \cdot |N_2| \cdot n_I + c)$. Given

the time cost for a prediction c_f (7.5 ± 0.8 ms, in our experiments) and that to back-propagate the output to the inputs c_b (7.8 ± 0.7 ms, in our experiments), the time complexity to generate a single DAX is instead $O(c_f + c_b \cdot |N_2| + c)$.

For the FFNN for COMPAS, the generation of the base for the pie chart (a one-time cost for χ) has a constant time complexity since it can be computed based on the input weights. Given the time cost for a prediction c_f (0.6 ± 0.1 ms, in our experiments) while we let c be any other (constant or negligible) computational cost, the time complexity to generate a single DAX is $O(c_f + c)$.

C Details of the human experiments

Figure 10 shows in details the background of the 72 workers of Amazon Mechanical Turk that participated in the experiments. The confidence intervals and the p-values describing the significance of a score wrt another one were computed using the independent two-tailed T-test statistics.

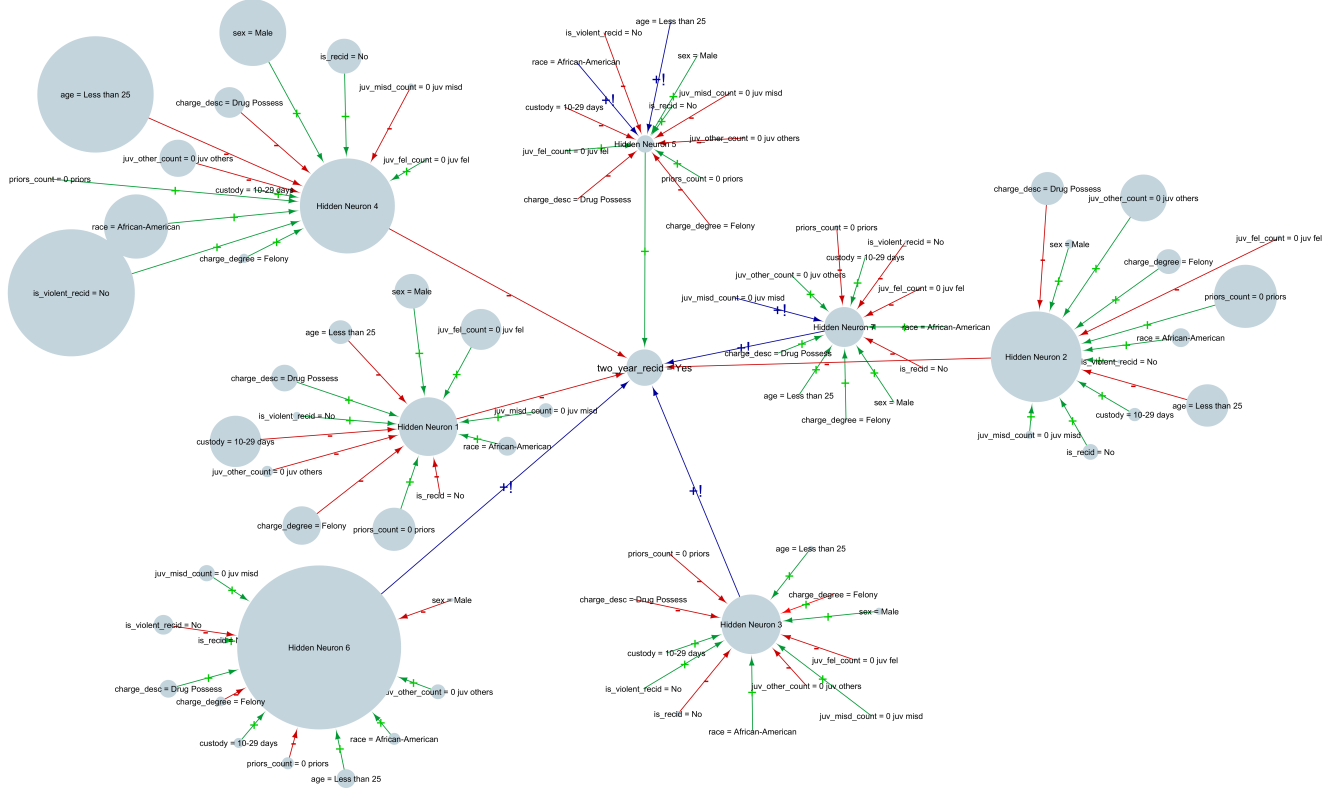


Figure 8: A bird's-eye view of a TAF (with 92 arguments) for a COMPAS sample. For each argument α , size corresponds to $\sigma(\alpha)$ and label to $\rho(\alpha)$. Red (-), green (+) and blue (!) arrows indicate, resp., attack, support, and critical support.

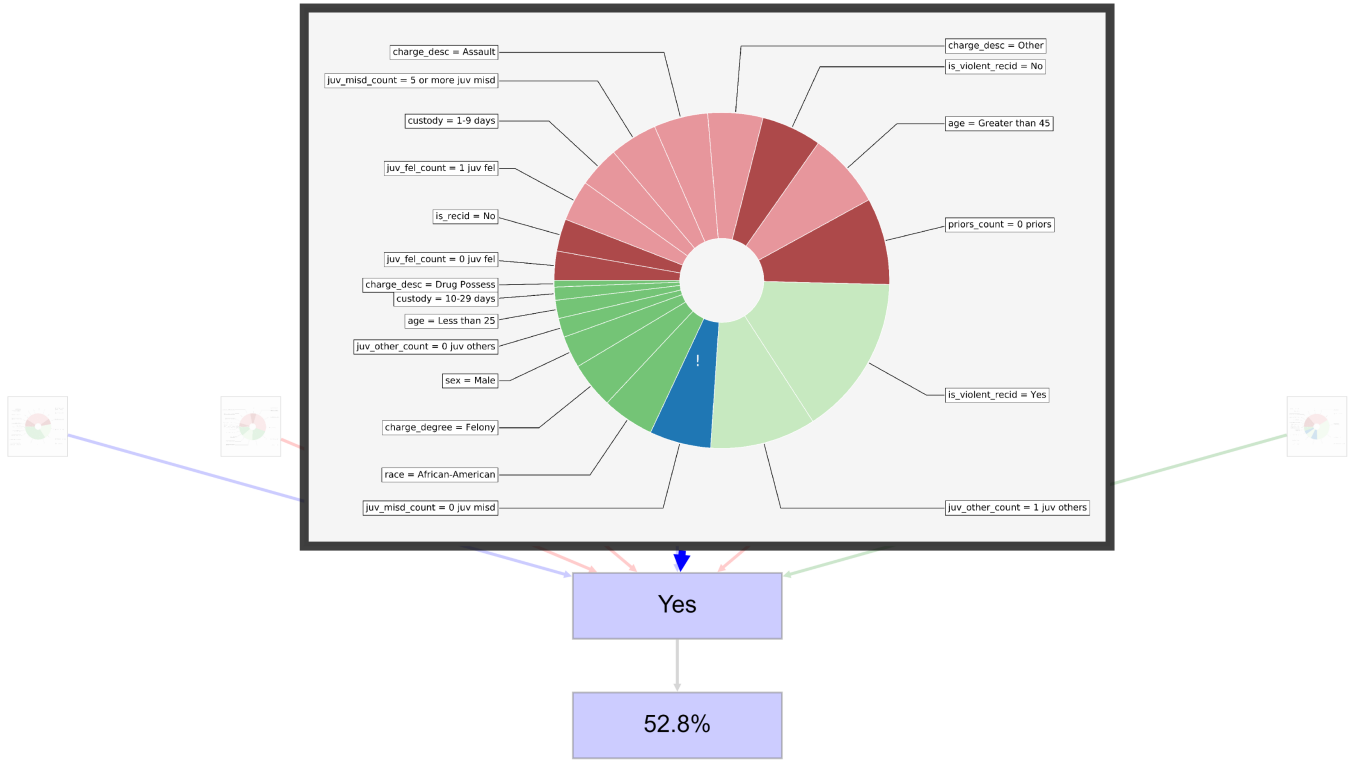


Figure 9: Graphical interactive DAX for a COMPAS sample. The (selected) pie chart represents, via χ : (i) an intermediate argument (hidden neuron) critically supporting the prediction 'Yes', as well as (ii) the strongest attackers, supporters and critical supporters (in dark red, green and blue, resp.) and the weakest attackers, supporters and critical supporters (in light red, green and blue, resp.) of this intermediate argument, chosen amongst the input arguments (features).

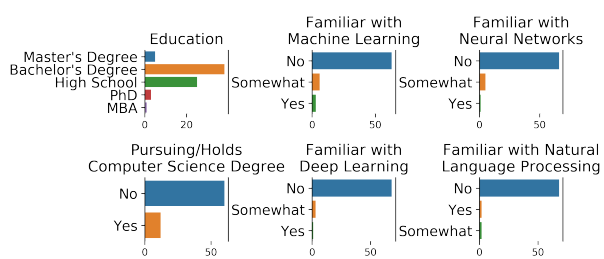


Figure 10: Backgrounds of participants